Review

Middle atmosphere research and radar observation

By Susumu KATO[*), †)]

Professor Emeritus, Kyoto University

(Communicated by Yoshibumi TOMODA, M. J. A.)

Abstract: Middle atmosphere research was found to be important, for the first time in the 1970s, with an information on possible atmosphere damage caused by human activity. International endeavors organized and carried out the Middle Atmosphere Program (MAP in 1982-1985). It was essential to understand dynamics of the middle atmosphere in MAP. In the early 1980s atmospheric gravity waves were found to play an important role in dynamics in the mesosphere, the upper part of the middle atmosphere. It was a good coincidence that atmosphere radars were found to be powerful for observing gravity waves. The MU radar of Kyoto University was constructed just on time in 1984. The facility, the best in the world for middle atmosphere observation, has been open for visiting scientists, domestic and abroad, even now, producing many excellent works. Of these works, this paper intends to review some important works done mainly by our Kyoto University radar group together with the basic knowledge of gravity waves.

Key words: Middle atmosphere; mesosphere; gravity waves(GW); the MU radar; turbulence.

1. Introduction. The middle atmosphere consists of the stratosphere and the mesosphere, extending from about 10 km to 90 km in heights. Below is the troposphere and above is the upper-atmosphere. Fig. 1 illustrates these atmospheres with temperature height-distribution which characterizes each atmosphere as decreasing with height in the troposphere, increasing in the stratosphere, decreasing in the mesosphere, increasing again in the thermosphere. The thermosphere is the beginning of the upper-atmosphere whose temperature tends to be constant with heights.

The middle atmosphere had remained little known until the 1970s when it was suddenly suspected that the exhaust gas of supersonic flight, which had been practical by then, would destroy the ozone layer in the stratosphere, thereby exposing all life on this planet to a dangerously excessive solar ultra-violet radiation reaching the ground. Later, this threat was found untrue. However, the middle atmosphere study was realized to be significant for practical as well as scientif-

ic purpose. An international collaborative program for middle atmosphere observation, which was called Middle Atmosphere Program (MAP), was planned and carried out in 1982-1985.

A basic requirement for successful MAP was to establish powerful ground-based remote sensing technique for observing the middle atmosphere structure and dynamics besides satellite remote sensing. Responding to this requirement, a powerful radar technique was developed for not only the middle atmosphere but also troposphere observation, resulting in constructing MSTR (Mesosphere, Stratosphere and Troposphere Radar) at various locations world-wide. This technique made it possible with good time- and height-resolution to observe winds, waves and turbulence.

There were two serious problems relative to the middle atmosphere in MAP. One was concerned with the ozone layer. Around the end of MAP the ozone hole in the Antarctic stratosphere was discovered and, since then up to now, the ozone hole has become the main problem about the ozone layer. The other was concerned with a peculiar mesosphere general circulation. This problem had been well known since the 1960s.[1)] It is the peculiar temperature and winds in the high latitude
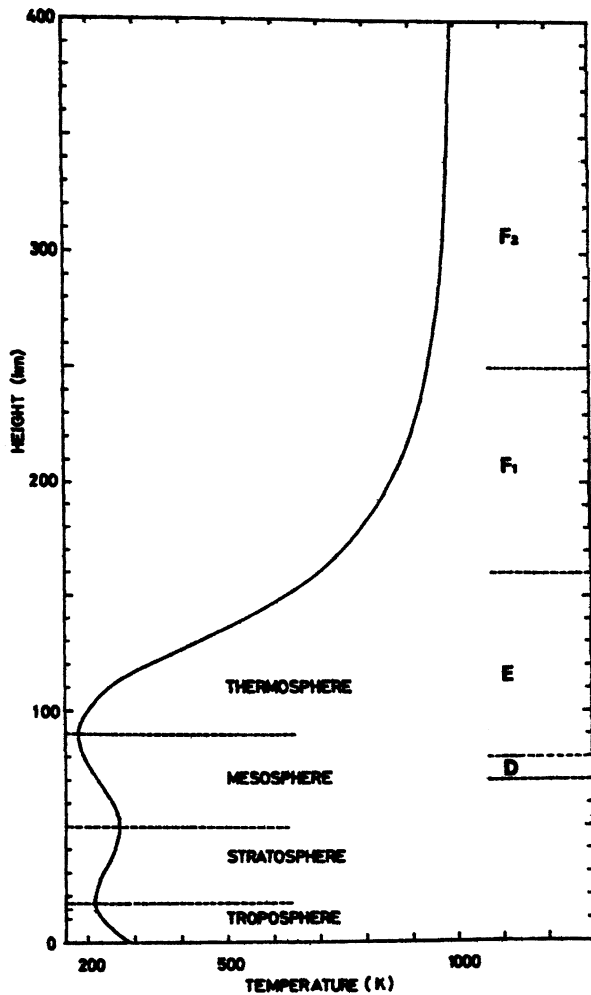
Fig. 1. Temperature distribution in the troposphere, the stratosphere and the mesosphere of which the last two in combination are called the middle atmosphere. Above the middle of the mesosphere from about 70 km up to 500 km is the ionosphere, consisting of four regions which are called, from below, the D, E, F_1, and F_2 layers. The F_1 and F_2 layers in combination are called the F layer.

mesosphere. The high-latitude mesosphere in winter is warmer than in summer. Further, winds around the mesopause (the mesosphere upper-boundary) are very weak, a peculiar behavior, which is inconsistent with what is expected from the thermal wind relation well-known in meteorology. It was found first by theory and soon later by radar observation that atmospheric gravity waves (hereafter, GW) play an important role in the mesosphere general circulation.

In this paper we are mainly interested to review as to how the second problem was pursued towards its solu-

tion and, further, how our successful mesosphere radar observation was done and the radar observation has been developed to the lower atmosphere i.e. the whole atmosphere observation.

2. Gravity waves (GW). Before explaining about the role of GW in the mesosphere general circulation, we must introduce the basic behaviors of GW which are atmospheric waves able to propagate horizontally and vertically. Whilst the GW propagation had fairly well been understood in the 1980s, the excitation was not well known until the 1990s. But now we understand that there are various ways of the excitation, as cumulus convection, topography through mountain waves, geostrophic adjustment and others.[2)-6)] Since the excitation of GW is not our present concern, any more detail of the works on the excitation will not be given below except that GW are excited in many ways and exist almost anywhere in the atmosphere.

The atmosphere in hydrostatic equilibrium tends to oscillate when disturbed. It is elementary to understand that when an air mass is a little displaced vertically, the mass expands adiabatically for upward displacement and contract for downward displacement. As a result, the displaced air mass tends to return to the original height because the air mass gets heavier than the ambient atmosphere for the upward displacement and gets lighter for the downward displacement, respectively. This means an existence of restoring force giving an oscillation of the atmosphere around the hydrostatic equilibrium altitude and the characteristic frequency is named the Brünt-Väisälä frequency N which is $(\gamma - 1)^{1/2}$ g/C where g is the gravity; γ the ratio of heat capacity between the constant pressure, C_p, and constant volume, C_v; C the sonic speed for isothermal atmosphere. Height distribution of N is shown in Fig. 2 where $T_B = 2\pi/N$ in minutes.[7)] The restoring force due to the gravity is fundamental to the existence of GW. On the basis of small perturbation theory, a set of linear dynamical equation of motion, continuity equation and thermodynamic equation can describe GW in a simple way and these equations are solved simultaneously with Fourier-transformation. The behavior of GW in isothermal atmosphere is given as[8)]

$$V_{x,z} = \exp(z/2H) \, v_{x,z} \qquad [1]$$

$$\text{where } v_{x,z} = A_{x,z} \exp\{i(\omega t - k x - m z)\} \qquad [1']$$

$$m^2 = \{(N^2/\omega^2) - 1\} \, k^2 - (\Pi^2 - \omega^2)/C^2 \qquad [2]$$
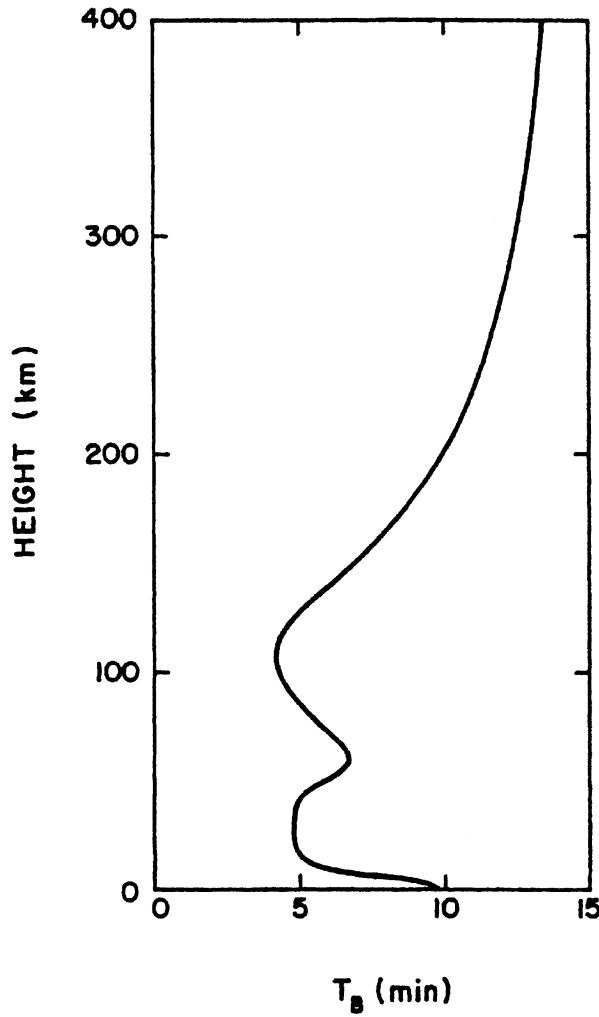
Fig. 2. Distribution of Brünt Väisälä period $T_B = 2\pi/N$ in minutes.

subscript o and superscript ' denote the static and perturbed part, respectively. GW have linear polarization in the (x-z) plane.

We consider now for $\omega \ll N$ and

$$|m| \gg |k|.$$

$$dv_x/dx + dv_z/dz \doteqdot 0 \qquad [3]$$

Note that [1], [2] and [3] are derived for a simple atmosphere model as assuming isothermal and plane atmosphere with no background wind and, further, the Coriolis force is neglected.

From [2], we readily understand that m becomes imaginary number in $\Pi > \omega > N$ where GW are not internal (external), unable to propagate vertically, but being trapped around the excited height, propagating only horizontally (x direction). With real-number for m we have internal waves able to propagate vertically. The internal waves consist of two modes, one being for $\omega < N$ and the other for $\Pi < \omega$; the former is of GW-mode and the latter is of acoustic-mode.

For $\omega \ll N$, we approximate [2] as

$$m^2 = (N^2/\omega^2)k^2 \qquad [3']$$

which is approximately valid for GW of our concern here. The vertical phase velocity C_z and group velocity C_g are given by [3'] as

$$C_z = \omega/m = \pm \, N \, k/m^2 \qquad [4]$$

$$C_g = \partial\omega/\partial m = -\, C_z \qquad [4']$$

In [1] and [1'] $V_{x,z}$ is GW velocity which consists of exponentially growing part $\exp(z/2H)$ and sinusoidal wave part $v_{x,z}$ with constant amplitude $A_{x,z}$; t is time; x and z Cartesian coordinates, horizontal and vertical, respectively; ω is the frequency; k and m are the wave number, horizontal and vertical, respectively. H is the atmospheric scale height as $(k_B \, T/mg)$ for isothermal atmosphere as assumed here, with the temperature T, the Boltzman constant k_B, the air molecule mass m. In [2] Π = acoustic low-cutoff frequency = $\gamma g/(2C) \doteqdot 1.1 \, N$.

As in [1], GW amplitude is *amplified* exponentially during propagation upward due to the decreasing ambient density, and this is the case also for relative pressure perturbation (p'/p_o) and density perturbation (ρ'/ρ_o) where p and ρ are pressure and density, respectively;

showing that the phase and group velocity are equal in magnitude but opposite in sign to each other.

Based on [1'] and assuming GW to be excited in the troposphere, $C_g > 0$, upward, and $C_z < 0$, downward.

The present linear approach gives infinite growth of the amplitude with z in [1], but non-linear effects in the real situation must give a saturation for the amplification unlike [1]. Though the saturation can not be correctly treated in our present linear treatment, we can suggest certain initiation of instability upon the saturation. Suppose that GW amplitude can attain a magnitude by amplification and be saturated through the vertical propagation with [1] as

$$|V_x| = N/|m| \qquad [5]$$

As is well known, if the temperature decreasing-rate with height Γ (temperature lapse rate) is $\Gamma > \Gamma_d$ where Γ_d is the adiabatic lapse rate as $\Gamma_d = g/C_p \fallingdotseq 9.8°/$ km for dry air, the atmosphere becomes convectively unstable. [5] suggests a situation close to the instability as follows: Since the equation of continuity gives, with $d\rho_o/dz = -\rho_o/H$,

$$\left| \omega\rho' \right| = (1/2) \left| V_z \right| (\rho_o /H) = (1/2) (N/\left| kH \right|) \rho_o \qquad [6]$$

the adiabatic relation exists between the density and temperature fluctuation as

$$T'/T_o = (\gamma - 1) (\rho'/\rho_o) \qquad [7]$$

Finally,

$$\left| \partial T'/\partial z \right| = \left| mT' \right| = (1/2)g/C_v =(1/2) \gamma \Gamma_d \qquad [7']$$

[7'] shows a situation fairly close to the convective instability threshold for $(1/2) \gamma \fallingdotseq 0.7$ with $\gamma = 1.3$. This instability may break GW into turbulence.

Another instability may also occur. If for GW the Richard number (Andrew et al.[9c]) $Ri = N^2/(dV_x /dz)^2$ is smaller than 0.25, a shear instability occurs. And only if Ri is more than unity, the situation is dynamically stable.

With [5] and [2]

$$Ri = 1/\{1+ 1/(4m^2 H^2)\} < 1 \qquad [8]$$

[8] shows that the GW is between unstable and stable. It implies that if V_x in [5] grows further with the vertical propagation as in [1], the shear may be intensified as to produce the instabilities producing turbulence.

Although the present approach for the GW saturation occurrence is fairly simple, we still could suggest that the saturation may give rise to the instabilities leading to turbulence. It is very important to realize that turbulence exists at any height where GW exist and are saturated. And GW seem to exist and are saturated anywhere in the atmosphere, so is turbulence anywhere. This understanding suggests possible radar-observation of the atmosphere almost at any height with turbulence as scatterers to be explained later.

GW interact with background winds and the GW interaction behavior is simply considered by Doppler-shifted frequency as $\omega \rightarrow (\omega - k U) = k(C_x - U)$ where C_x is the x-component of phase velocity. Then, [3'] is transformed to

$$m^2 = N^2 /(C_x - U)^2 \qquad [9]$$

[9] implies that [5] is equivalent with $\left| V_x \right| = \left| C_x - U \right|$.

Instabilities, no matter with convective or shear instability, may release the GW momentum to the background winds, accelerating or decelerating winds. A rigorous treatment of the GW momentum release is to consider divergence of the GW momentum flux as $\langle \rho_o V_x V_z \rangle$ where $\langle \ \rangle$ denotes time-mean quantity (Andrew et al.[9a]) Since

$$\rho_o \partial U/\partial t = -\partial \langle \rho_o V_x V_z \rangle /\partial z \qquad [10]$$

where U is the background winds along the x direction, the right-hand side of [10] turns to be

$$\{ -(m/k) \rho_o \left| V_x \right|^2 \} \qquad [10']$$

with [1'] and [3], provided that, as in the WKB approximation, m is assumed constant. Since GW are excited in the lower atmosphere propagating upwards, $m < 0$ by [4] as well as [4'], the GW momentum flux accelerates U along k. However, in the instability region m changes rapidly with height and [10'] cannot be correctly applicable in the region which is of our concern. Thus, it is essential to observe directly $-\partial \langle \rho_o V_x V_z \rangle /\partial z$. Recently, interesting simulation of the non-linear process of GW breaking has been done.[10]

GW, which play a role in the mesosphere circulation, are, mainly, long-period GW called inertia GW[11] which have much lower frequency than that discussed above and affected by the earth's rotation i.e. the Coriolis effect giving more complex dispersion than [2]. Inertial GW are not linearly polarized but elliptically polarized. The Coriolis effect is important for GW with period near 12 hrs at the pole, increasing with decreasing latitudes as 24 hrs at 30° of latitude and disappears at the equator. The earth as a sphere, not considered here, is also effective with increasing periods, generally implying increasing wave-lengths. Nevertheless, the essence of GW behavior of our present concern remains the same between our present simple approach and more complicated approach for understanding the interaction of GW with the background winds. We will follow the simple approach in understanding physical mechanism of the GW breaking for the mesosphere circulation peculiarity as above-mentioned.

3. Mesosphere general circulation. Fig. 3 (a)

and (b) show, respectively, zonal-mean temperature and the corresponding zonal-mean zonal winds in the atmosphere.[1] These figures are summary of global observation with rawinsodes as well as special high level balloons up to the middle stratosphere. Beyond this height rockets (meteorological and of other types) were used in observation. The peculiar fact is about temperature and winds around the mesopause in high latitude, as noted in Section 1. This peculiarity had remained open question for more than two decades until the 1980s.

Besides the anomolous mesopause temperature as warmer in winter than in summer as in Fig. 3(a) there exists a weak wind region in Fig. 3(b), where the wind velocity contour is closed above about 65 km height, is not consistent with that expected from the thermal wind relation. The thermal wind relation is well-known in meteorology, showing that the geostrophic balance is maintained between the pressure gradient and the Coriolis force except for the equatorial region (e.g. see Kato[12a]) as

$$\partial U/\partial z = -(g/2\Omega)\ (1/\sin\phi)(1/T_o)(\partial T_o/a\partial\phi)\quad [12]$$

where Ω is the earth's rotational speed. ϕ the latitude, a the earth's radius. The stratosphere (below 50 km height) temperature distribution along latitude in Fig. 3 (a) and [12] makes us expect that zonal winds in the mesosphere both in winter and summer should increase monotonously with height, the expectation, which is inconsistent with the observed fact as shown in Fig. 3 (b). This suggests that some extra force exists in the mesosphere, disturbing the geostrophic balance between the Coriolis force and pressure gradient force, the balance, on which [12] is based.

The new force, if ever exists, acts as a braking force against the mesospheric zonal winds. In order to have a stationary zonal wind system in the mesosphere the braking force has to be balanced with an additional Coriolis force which is to be produced by an extra meridional wind. Considering that the direction of zonal winds is eastwards in winter and westwards in summer and the braking force must be opposite to the zonal wind directions, the meridional wind must flow from the summer hemisphere toward the winter hemisphere, thereby producing the additional Coriolis force which is eastwards in winter and westwards in summer in balance with the braking force.

Further, the extra meridional wind results, due to continuity of the meridional wind flow, in producing an upward flow in summer and a downward flow in winter in the mesosphere. This vertical flows cause adiabatic compression in winter and adiabatic expansion in summer in the mesosphere. This can explain why the peculiar temperature and weak winds occurs in the mesosphere.

Matsuno (1982),[13] Holton (1983)[14] and Geller (1983)[15] put forwards an idea postulating GW to be breaking into turbulence, releasing negative momentum to winds and working as the braking force against winds. The idea is based on a very similar idea once used for explaining QBO (Quasi Biennial Oscillation) in the equatorial stratosphere where, besides GW, the Kelvin waves are playing a role (Andrew et al.[9b]).

It is fairly plausible to assume an excitation of GW traveling east- or west-wards somewhere in the troposphere. These waves travel upwards, increasing amplitudes as in [1] and suffering Doppler shift of the original frequency relative to the ambient winds (Fig. 3(b)) to change m as in [9]. Between GW traveling eastwards and that traveling westwards, m becomes different. GW traveling in the wind direction tend to have larger m whilst those traveling against the wind direction tend to have smaller m as in [9]. The former have slower vertical group velocity than the latter as in [4'] and, with shorter vertical wave-length (larger m), may suffer more dissipation by eddy viscosity due to turbulence.[13] Instabilities as [7'] and [8] may more easily occur for larger m and even the critical level may arise with $C_X = U$ which is possible only for GW traveling in the direction of winds (Andrew et al.[9a]). Thus, we can expect for GW traveling against winds to have more chances to be able to survive dissipation during the propagation before reaching the mesopause where the GW may break into turbulence, braking the zonal winds by releasing the GW momentum to the zonal winds.

4. Radar observation. *4.1. Principle of radar observation and existence of turbulence.* Radar echo from the mesosphere was detected by Woodman and Guillen (1974[16]) during the time of observing the ionosphere with the Jicamarca Radar in Peru. The radar echo was Doppler-shifted, seemingly to show mesospheric winds. Later it was found that the radar pulse scatterer is the mesosphere turbulence which co-moves with the background winds as shown by the observed Doppler shift.

As understood through discussion in Section 2 and 3, the GW breaking produces turbulence in the mesosphere. This idea presented a possibility of mesosphere remote sensing by radars. On the basis of the technique
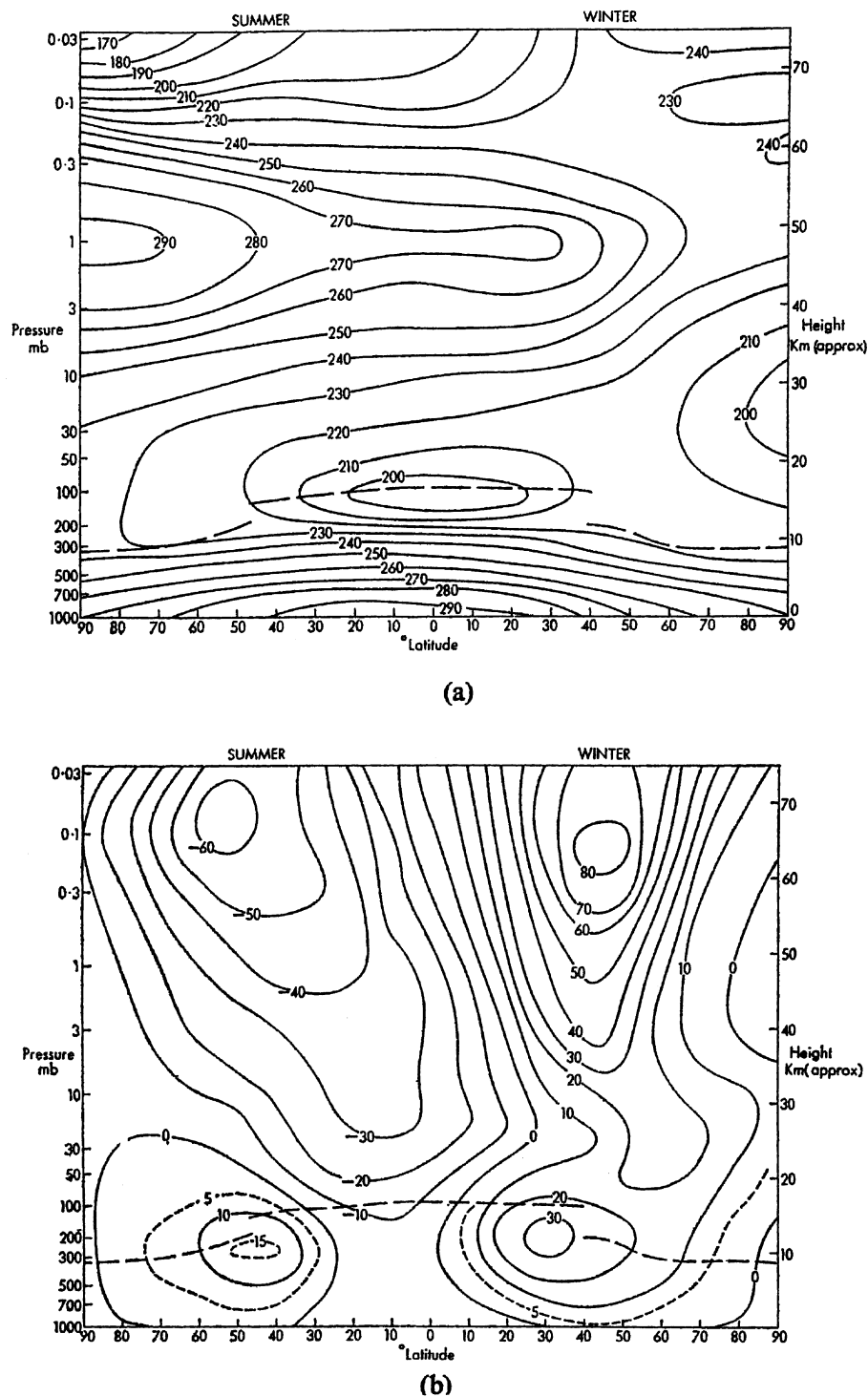
Fig. 3. Zonal-mean temperature and zonal winds (global observation summary). (a) Zonal-mean temperature (in degrees) distribution with height and latitude in the solstice season, one hemisphere in summer (in left-hand side) and the other in winter (in right-hand side). (b) Same except for zonal-mean zonal winds (positive for eastward and negative for westward, in m/s): See the mesospheric peculiarity above about 60 km height. Broken lines show the tropopause, the upper-boundary of the troposphere.

we saw construction of MST (Mesosphere Stratosphere Troposphere) radars which suits the observation of dynamics of the MST region which is full of turbulence.

The radar observation is based on the tracking of turbulence which results in perturbation of the radio refractive index scattering the radar echo. Radio refractive index Λ [17] is given as

$$\Lambda = 1 + 3.73 \cdot 10^{-1} \ (e/T^2) + 7.76 \cdot 10^{-5} \ (P/T) - (N_e/2N_c) \qquad [13]$$

where e is the partial pressure of water vapor in mb, P the pressure same to p expressed in mb, N_e the electron number density per m^3, N_c the critical plasma density given as $N_c = 1.24 \cdot 10^{-2} \ f^2 \ m^{-3}$ with f as the radio wave frequency per sec. $\delta\Lambda$, perturbed Λ, generates the scattering of radar pulses in the presence of turbulence.

Based on the assumption as div $V = 0$ and isotropic turbulence, the turbulence velocity spectrum $E(\kappa)$ was theoretically obtained in the 1950s by Batchelor [18] as

$$E(\kappa) \propto \kappa^{-5/3} \qquad [14]$$

where κ is the wave number of turbulence: [14] is valid in the inertial subrange of turbulence with $\kappa < \kappa_d$ where κ_d gives the minimum scale of turbulence or the boundary between the turbulence inertial-subrange and viscous subrange. The theory gives

$$\kappa_d \propto \mu^{-3/4}$$

where μ is the kinematic viscosity inversely proportional to the atmosphere density and increases exponentially with height; accordingly κ_d decreases with height. For $\kappa > \kappa_d$, in the viscous range

$$E(\kappa) \propto \kappa^{-7} \qquad [15]$$

Note that [14] and [15] show the turbulence velocity spectrum integrating for all direction of κ and the spectrum for each direction of κ, Ψ, is given

$$\Psi = E(\kappa)/(4\pi\kappa^2) \propto \kappa^{-11/3} \quad \text{for } \kappa < \kappa_d \qquad [14']$$

$$\propto \kappa^{-9} \quad \text{for } \kappa > \kappa_d \qquad [15']$$

In spite of div $V = 0$ the equation of continuity gives a density perturbation in the presence of vertical gradient of the atmosphere density as

$$\partial\rho'/\partial t = - V_z \ (d\rho_o /dz) \qquad [16]$$

where the vertical density gradient is mainly due to the ambient density gradient depending only on z. Thus, it is understood with [16] that the atmosphere density perturbation is produced by the velocity turbulence, obtaining the density perturbation spectrum which is same to the velocity turbulence spectrum [14'] and [15'].

In [13] the second term gradient is due to (e/T^2) in the troposphere and the perturbed (e/T^2) is produced by V_z as ρ' in [16]. The third term gradient is due to ρ in the stratosphere and just follows [16]. Note that the middle and upper stratosphere echo is extremely weak and can be observed only with very powerful radars [19] The last term gradient is by N_e in the mesosphere where the N_e perturbation occurs distinctly from other lower atmospheres because of the existence of electro-magnetic effect on electrons.

First, note that ions co-move with neutral particles through collisions with neutral molecules up to the lower thermosphere whilst electrons move very differently above 60 km under strong control by the geomagnetic field $\boldsymbol{B}_o$. Electrons only are responsible for scattering radio waves. Next, it must be understood that any difference in motion between ions and electrons along grad N_e = grad $N_i \neq 0$, where N_i is ion number density would immediately set up an intense electric polarization-field which causes electrons and ions to co-move *along the gradient of N_e*. However, orthogonally both to the polarization field and $\boldsymbol{B}_o$, the Hall drifts take place, moving electrons and ions differently, but the drifts (orthogonal to the gradient of Ne). have no divergence, as understood by simple electrodynamic consideration (Kato [12b]). Therefore, besides the original perturbation along (grad N_e) no electron density perturbation is produced. Thus, any refractive index perturbation in [13] follows the spectra in [14'] and [15'].

In order to get the radar echo scattered by turbulence, in back-scattering, one half of radar wavelength size of the turbulence spectra $\Psi(\kappa)$ in [14'] contributes to the radar pulse scattering. [20] The half of the radar wavelength must be in the turbulence inertial-subrange bounded by κ_d which is proportional to the atmosphere density.

Consider that half the radar-wavelength be in the inertial subrange of turbulence at some height. This favorable wave-length approaches the inertial subrange end with increasing height with decreasing κ_d. Finally, at some higher altitude the half of radar wave-length
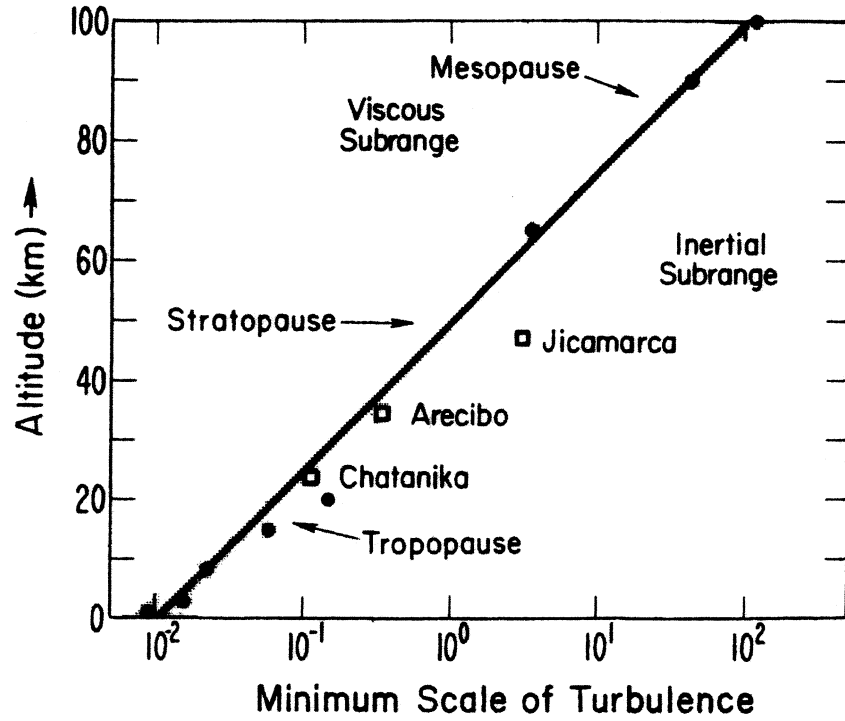
Fig. 4. Minimum scale of turbulence $\lambda_{\min} = 5.92/\kappa_{\mathrm{d}}$, in m (Balsely and Gage, 1980,[17]). The solid circles and the open squares denote the maximum height of observed atmospheric echoes for radars operating at different frequencies. The open squares are used particularly for well-known radars. with their locations.

leaves the inertial subrange, entering the viscous subrange, resulting into no radar echo because of insufficient turbulence spectrum intensity in the viscous subrange as in [15']. The situation for various wavelengths is illustrated in Fig. 4 which shows the minimum scale of turbulence $\lambda_{\min}$ in m; although the turbulence theory uses fairly unrealistic assumptions as div $V = 0$, Fig. 4[17] shows that the fitting to the radar experimental results (the thick diagonal, giving $\lambda_{\min} = 5.92/\kappa_{\mathrm{d}}$) is fairly consistent with the theoretical result $\lambda_{\min} = 2\pi/\kappa_{\mathrm{d}}$.

The turbulence moves with background winds with velocity determined by the maximum of the radar echo's Doppler spectrum; the spectrum spreading is due to the turbulence random motion. At 100 km the minimum scale of turbulence was found to be about 100 m. Thus, besides winds the radar observation gives an information on the turbulence property in the atmosphere from the ground up to 100 km height.

4.2. MU radar observation of GW. Desirable MST radar specification may be as follows: The wave-length λ must be $(1/2)\lambda > 2\pi/\kappa_{\mathrm{d}}$ i.e. in the inertia subrange in the MST region. Besides this condition, our desirable λ

must receive the echo power as much as possible. Considering the radar scattering cross-section,[20] the echo power is proportional to $\lambda^{-4} \langle \delta\Lambda \rangle^2$ times the turbulence spectra Ψ in [14']. The power dependency on λ varies from M (mesosphere) to ST (stratosphere and troposphere).

For M , as in [13], Ne-term is proportional to λ^2 and the radar echo power is proportional to

$$\lambda^{-4} \langle \delta\Lambda \rangle^2 \Psi(k) \propto \lambda^{11/3} \qquad [17]$$

where $k = 4\pi/\lambda$. For ST with $\langle \delta\Lambda \rangle$, independent from λ, the echo power is proportional to

$$\lambda^{-4} \langle \delta\Lambda \rangle^2 \Psi(k) \propto \lambda^{-1/3} \qquad [18]$$

Under the circumstances it is recommended for MST radars to use λ to be several meters or around 50 MHz as frequency (See Fig. 4). A higher frequency (GHz) is suitable for the lowest atmosphere (the planetary boundary layer) observation as understood with [18].

Fig. 5. Bird-eye view of the MU radar in Shigaraki Shiga in Japan. In the circular antenna area with diameter of
about 100 m there are 475 of 3-element crossed-Yagi which are arrayed to make up 25 groups, each group with
19 elements (arrayed in hexagon-shape area) and each element has a transmitter-receiver module. The total sys-
tem is computer-controlled so as to make it possible to steer the beam to almost any direction within 30° of
zenith angle in an interpulse period of one millisecond. All of the modules are shared and stored in the 6 booths
around the antenna area. The area is valley-shaped surrounded by the metal-net fence as tall as 10 meter pre-
venting radar waves from being transmitted to and returned from near-by mountain (as clutters) in low eleva-
tion angle. The shortest range resolution is about 150 m.

The MU radar (the middle and upper atmosphere radar[21]) was completed in its construction in Shigaraki about 50 km south-east of Kyoto in 1984 (Fig. 5) as Kyoto University facility which is open for visiting scientists domestic and from abroad. The facility has a fairly high sensitivity $5 \cdot 10^8$ W m^2 (defined as the average output power times antenna area in terms of W m^2) and is able to receive, besides MST turbulence echoes, ionosphere incoherent-scatter echo due to the ionosphere plasma ion-acoustic waves though only with a few hrs integration.[22] Among MST radars, the MU radar is unique in that the facility can swing the radar beam toward almost any direction within 30° from the zenith in milliseconds, with active antenna array system[23] and is able to track atmosphere motion in rapid fluctuation as GW.

Soon after inception of the MU radar operation, we were successful to observe precise behaviors of meso-spheric GW which had little been understood until then.[24] Fig. 6 shows the result of the MU radar observation of radial winds with beam angle from the zenith 10° to the south. The observed GW, with period between 6-16 min in 70-78 km heights, shows a peculiar behavior in that there is almost no phase variation with height below and above 73 km height where the amplitude becomes minimum and a phase reversal occurs, probably implying an instability taking place in 70-78 km region. Note that we confirmed carefully the phase reversal by comparing the phase of GW between both sides of 73 km in detail although not shown here. Of the interesting observed fact our correct understanding about the resonance-like oscillation with a frequency close to N is still open to question.

Another important contribution of the MU radar observation to GW research in an early period of the MU radar operation was the determination of GW saturation
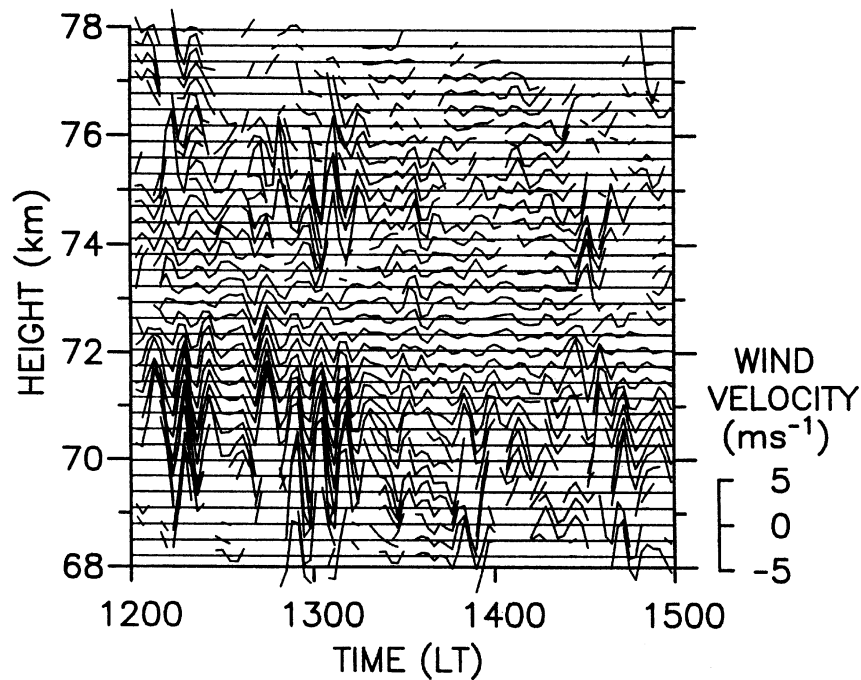
Fig. 6. Radial wind fluctuation of GW with period in 6-16 min on 8 Feb. 1985.[24]

spectrum, an issue which had been controversial. The MU radar observation[25] was successful to obtain GW saturation spectrum in all MST regions. Results are illustrated in Fig. 7. It should be remarked that the spectrum observed by the MU radar behaves similarly among the M, S, and T regions; mathematically the spectrum approximates to $N^2/(6 \ m^3)$ for m larger than about $3,5 \cdot 10^{-4}$ (c/m) consistent with model by Smith *et al.*[26] Note that [5] can explain qualitatively the GW saturation which results in instabilities but we can hardly explain any definite association between [5] and Smith' model or the observed saturation spectrum.

The observed fact that GW in the MST region follows the universal saturation spectrum implies that GW break is taking place and producing turbulence similarly in the whole MST region. This is an important discovery, having demonstrated the MST radar observation significance. It seems important, as noted above in relation to Λ in [13], to mention that from the middle and upper stratosphere no echo has been received so far with the MU radar as well as other facilities in the mid-latitudes. But Maekawa *et al.* in 1993[19] have received echoes with the Jicamarca radar in Peru in the equatorial latitudes.

In order to solve the peculiar mesosphere circulation problem which had remained unsolved for a long time we had to observe GW braking the mesopause zonal winds. It was necessary to check observationally whether [10] gives deceleration of U as much as the theory requests. In winter U is eastward and the braking must have a westward momentum flux (due to westward traveling GW as in [10']), magnitude of which must decrease with height, showing an absorption of the momentum by winds. In summer the situation must be just opposite.

An important observation method on this issue was developed by Vincent and Reid in 1983.[27] Fig. 8 illustrates the principle of their method where GW are assumed to propagate in the diagram plane and the GW has a wavelength which is long enough to neglect difference in phase of the GW observed between the two beams along θ symmetrical to the zenith where θ is the zenith angle of radar beam. Denoting the observed GW along θ directions, respectively, as $V_{R1,2}$ (radial velocity, positive for outward)

$$V_{R1,2} = \pm V_x \sin\theta + V_z \cos\theta \qquad [19]$$

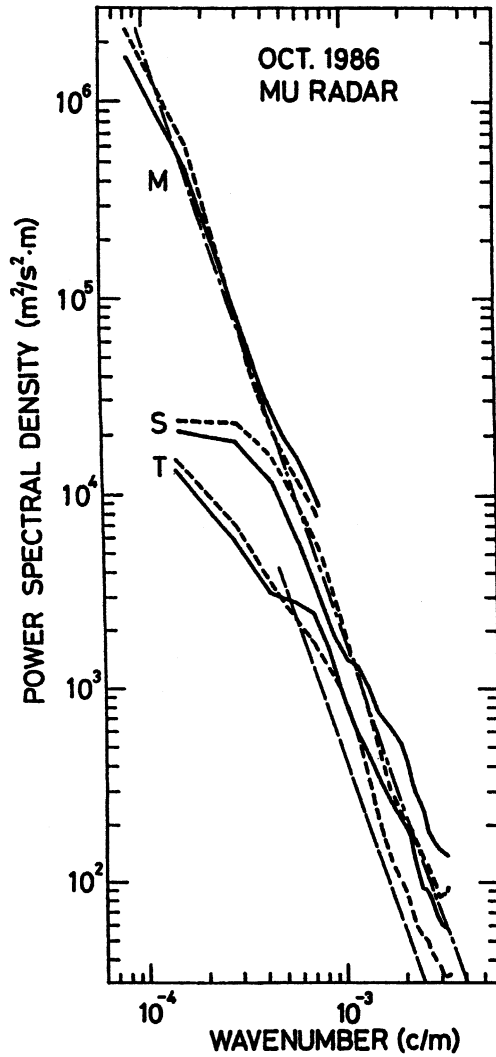where $\pm$ refers to $V_{R1,2}$ respectively. From [19]

Fig. 7. GW saturation spectrum. M, S and T stand for the mesosphere, stratosphere and troposphere, respectively; solid curved-lines are for the zonal and dotted curved-ones for the meridional winds; dot-dashed straight lines give the model spectra (see text).

$$V_{R1}^{2} - V_{R2}^{2} = 4 V_x V_z \sin \theta \cos \theta$$

$$V_x V_z = (1/2)(V_{R1}^{2} - V_{R2}^{2})/\sin 2\theta \qquad [20]$$

[20] gives directly the momentum flux without obtaining separately $V_{x,z}$, although in real observation a proper averaging is done for $V_{R1,2}$.

Our observation of GW based on [20] with the MU radar proved successfully a deceleration of zonal winds as illustrated in Fig. 9.[28] The observation was done routinely, monitoring winds from 60-90 km for about four
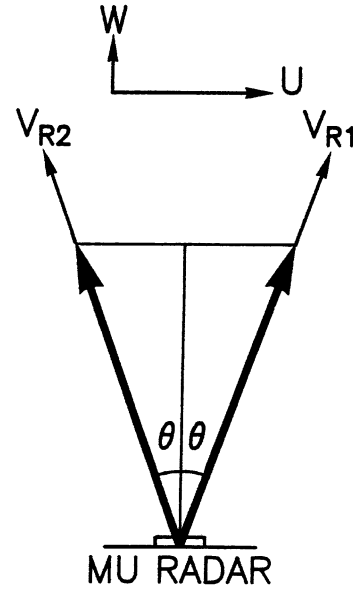

Fig. 8. Principle for GW momentum flux observation. MU radar beam is slanted by θ symmetrically to the zenith: W and U are GW (for V_z and V_x in text, respectively) vertical and horizontal velocities, respectively; $V_{R1,2}$ are velocities along the radar beam (positive for outwards).
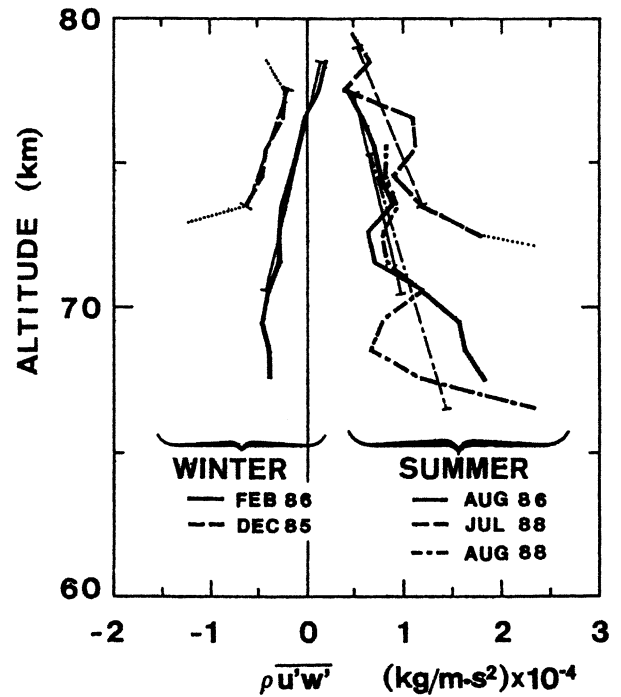

Fig. 9. GW eastward momentum $\langle \rho_o V_x V_z \rangle$ observed with the MU radar in summer (right-side) and winter (left-side). In the figure ρ_o is obtained from a standard model, V_x and V_z denote u and w in text, respectively and time average $\langle \ \ \rangle$ in text is shown by $^{-}$. All straight lines (solid, dotted broken and chain) show the best fit for the vertical gradient of $\langle \rho_o V_x V_z \rangle$.

days in every month from December 1985 to December 1988. Radial winds along the radar beam were observed with time and range resolution as 145 sec and 600 m, respectively.

During daylight hours the radar beam was steered to four oblique directions, north-south, east-west with 10° zenith angle and the vertical direction. For each day the observed velocity was frequency-spectra-analyzed. Only GW with periods between 5 min-2hrs were used to obtain the momentum flux. Whilst northward momentum flux $\langle V_y V_z \rangle$ was about 2 m^2 sec^{-2} and fluctuating in sign throughout one year, eastward momentum flux $\langle V_x V_z \rangle$ was –1.5 m^2 sec^{-2} in winter and +2 m^2 sec^{-2} in summer, without sign fluctuation. Since zonal winds in winter is eastward and that in summer is westward, the observed GW zonal momentum flux was directed to be opposite to zonal winds in both winter and summer, the result, which was consistent with theoretical expectation.[13)-15)] The observed result of GW zonal momentum flux varying with height gave the best-fitting straight lines for $-\partial(\rho_o \langle V_x V_z \rangle)/\partial z$ which showed deceleration as +7.2, +12.8 and +9.4 m/sec/day over 70-77 km in Aug. 1986, over 73-79 km in July 1988 and 66-75km in August 1988, respectively and –7.6 and –11.0 m/sec/day over 70-78 km in Feb. 1986 and over 73-77 km in Dec. 1985. However, it was found that the observed deceleration was smaller than that obtained by simulation which was based on theory by Holton and Wehrbein.[29)] Later, analysis of the GW momentum flux and its vertical derivative with the data in October 1986, June 1987, and July 1990 for GW with period over wider range as 8-0.5 hrs[11)] was attempted to find that the deceleration was much larger than that with the shorter period range and even larger than that theoretically predicted. Other observation (e.g. Ref. 30)) also gave similar or larger deceleration values of zonal winds. Thus, the outstanding problem for many years on the general circulation of the mesosphere at last saw a solution, theoretically and observationally. Now it is known that even in the Arctic mesosphere (Private Communication, Tsutsumi *et al.* 2005) GW propagate mainly against zonal winds in all seasons, very probably working as drag forces.

Two decades since MAP, the MU radar now is still active with fairly constant up-grading of the system. However, GW research is now facing a new situation as to find how much GW may survive the mesosphere breaking and travel further above 100 km height into the thermosphere. In the thermosphere with increasing kinematic viscosity, GW tend to dissipate around 300 km as discussed by Hines.[31)] Since the thermosphere is ionized, ions also behave as a drag force for motion. Still, certain instability also may develop due to decreasing density. Nevertheless the GW momentum release upon the dissipation and possible breaking in the thermosphere has been little understood, an important issue, which has to be investigated both theoretically and observationally.[32),33)] This presents a challenge to develop a new observation system of thermosphere GW besides the MU radar. In order to observe neutral particle motion as GW in the ionized thermosphere, in principle, optical radars as lidars are suitable but not yet powerful enough for thermosphere observation. Passive facilities as Fabry-Perot Interferometer[34)] are unable to observe height distribution. Incoherent scatter radar observation[22)] is only able enough for the purpose except the lower thermosphere with disturbing meteor echoes etc. It is desirable to find a novel idea for solving the problems.

4.3. Radar observation of the lower atmosphere. Besides the saturated spectrum observation, the MU radar is powerful in observing dynamics in the MST region in general with the fast beam-steering ability. Among others, vertical air-motion observation is possible, a unique observation, which has a significant breakthrough to the conventional meteorology observation with rawinsondes which are unable to observe vertical winds. The MU radar was successful to precise three-dimensional air motions over the Baiu front.[35)]

Another distinct contribution with the MU radar is to observe rain drops in 3-dimensional motion. The observation is useful to know rain-drop size distribution important for cloud physics but meteorological radar can track only rain-drop being transported by unknown winds vertical and horizontal. Now the MU radar is able to observe 3-dimensional winds by tracking turbulence in the background winds in addition to tracking raindrops as meteorology radars.[36)]

Another radar of fast beam-steering system was constructed by Kyoto University at the equator in Sumatra Indonesia in 2002 as illustrated in Fig. 10. This is the Equatorial Atmosphere Radar (EAR: Fukao *et al.*[37)]). Soon after the MU radar completion we were interested in radar observation of the equatorial atmosphere which is most intensively heated on this planet in the Indonesian Archipelago or the maritime continent driving the global atmosphere circulation. There are many interesting yet little-understood issues about equatorial-atmosphere dynamics as equatorial waves, which suit our radar observation. Our intense efforts for many years came to fruition, in 2002, in the construction of the EAR which is about $\frac{1}{10}$, in radar sensitivity, of the MU radar

Fig. 10. EAR (the equatorial atmosphere radar) at Kototabang near Bukittingi, Sumatra Indonesia. Besides EAR, there are many other facilities for observing the equatorial atmosphere and for satellite-communication with Japan (not shown in the figure).

and is able only to observe the troposphere but equally excellent in beam-steering-ability as the MU radar system. Also the system is being improved with adding a multi-static configuration.[38]

5. Concluding remarks. Research of the middle atmosphere, which was once the last unknown region of the earth's atmosphere, has now established a basis to consider the whole atmosphere to be one system, each part of which, as the troposphere, stratosphere, mesosphere and upper-atmosphere, couples with each other dynamically through various vertically traveling atmosphere waves. Of these waves the present paper is concerned particularly with GW which are now understood to be important not only academically but also practically for improving weather forecast.[39]

Doppler radars have been found to be powerful for GW observation and now applied widely for dynamics observation in all region of the atmosphere. The radars can receive echoes not from clouds but from atmosphere turbulence which exists at any heights; generally we call the radars clear-air radars or wind-profilers. In free atmosphere above the planetary boundary layer GW breaking causes turbulence to occur anywhere. Many small radars of this type (using GHz radio-wave) only for lower troposphere observation are also now deployed at many locations for operational meteorology-observation in the U.S.A, Japan and other countries.[40],[41]

Unlike tracking turbulence, a similar type of pulsed Doppler radars, designed for mesosphere observation with VHF-frequency radio waves, can track meteor trails which constantly appear in 80-100 km heights, moving with local winds. The meteor echoes are so intense than turbulence echoes that meteor radars, much smaller systems than MST radars, can suit a long period observation of the mesosphere and the lower thermosphere, useful for climatological study of atmospheric waves.[42]

The present paper may demonstrate that the wind-profilers (clear air radars), symbolized by the MU radar, have contributed much so far and will do so in future to the research not only for the middle atmosphere but also the whole atmosphere.

References

1) Murgatroyd, R. J. (1969) The structure and dynamics of the stratosphere. The Global Circulation of the Atmosphere (ed. Corby, G. A.). British Meteorological Society, London, pp. 159-195.

2) Sato, K. (1989) An inertial gravity wave associated with a synoptic-scale pressure trough observed by the MU radar. J. Met. Soc. Japan **67**, 325-334.

3) Fritts, D. C., and Luo, Z. (1992) Gravity wave excitation by geostrophic adjustment of the jet stream part I, Two-dimensional forcing. J. Atmos. Sci. **49**, 681-697.

4) Sato, K. (1994) A statistical study of the structure, saturation, and source of inertio-gravity waves in the stratosphere observed with the MU radar. J. Atmos. Terr. Phys. **56**, 755-774.

5) Sato, K., Hasiguchi, H., and Fukao, S. (1995) Gravity waves and turbulence associated with cumulus convective convection observed with the UHF/ VHF clear-air Doppler radars. J. Geophys. Res. **100**(D4), 7111-7119.

6) Satomura, T., and Sato, K. (1999) Secondary generation of

gravity waves associated with the breaking of mountain waves. J. Atmos. Sci. **56**, 3847-3858.

7) Liu, C. H., Klostermeyer, J., Yeh, K. C., Jones, T. B., Robinson, T., Holt, O., Leitinger, R., Ogawa, T., Sinno, K., Kato, S., Ogawa, T., Bedard, A. J., and Kerseley, L. (1982) Global dynamic responses of the atmosphere to the eruption of Mount St. Helens on May 18, 1980. J. Geophys. Res. **87**, 6281-6290.

8) Hines, C. O. (1960) Internal atmospheric gravity waves at ionospheric heights. Can. J. Phys. **38**, 1441-1481.

9) (a) Andrews, D. G., Holton, J. R., and Leovy, C. B. (1987) *In* Middle Atmosphere Dynamics. Academic Press, Orlando-San Diego-New York-Austin-Boston-London-Sydney-Tokyo-Toronto, p.177 and p. 183; (b) Andrews, D. G., Holton, J. R., and Leovy, C. B. (1987) *In* Middle Atmosphere Dynamics. Academic Press, Orlando-San Diego-New York-Austin-Boston-London-Sydney-Tokyo-Toronto, pp. 314-331; (c) Andrews, D. G., Holton, J. R., and Leovy, C. B. (1987) *In* Middle Atmosphere Dynamics. Academic Press, Orlando-San Diego-New York-Austin-Boston-London-Sydney-Tokyo-Toronto, p. 338.

10) Fritts, D. C., and Alexander, M. J. (2003) Gravity wave dynamics and effects in the middle atmosphere. Rev. Geophys. **41**, 1003.

11) Nakamura, T., Tsuda, T., Yamamoto, M., Fukao, S., and Kato, S. (1993) Characteristics of gravity waves in the mesosphere observed with the Middle and Upper Atmosphere Radar I. Momentum flux. J. Geophys. Res. **98**, 8899-8910.

12) (a) Kato, S. (1980) *In* Dynamics of the Upper Atmosphere. Center for Academic Publications Japan, Tokyo, D. Reidel Pub. Co., Dordrecht, p. 12; (b) Kato, S. (1980) *In* Dynamics of the Upper Atmosphere. Center for Academic Publications Japan, Tokyo, D. Reidel Pub. Co., Dordrecht, pp. 141-150.

13) Matsuno, T. (1982) A quasi one-dimensional model of the middle atmosphere circulation interacting with internal gravity waves. J. Meteorol. Soc. Jpn. **60**, 215-226.

14) Holton, J. R. (1983) The influence of gravity wave breaking on the general circulation of the middle atmosphere. J. Atmos. Sci. **40**, 2497-2507.

15) Geller, M. A. (1983) Dynamics of the middle atmosphere. Space Sci. Rev. **34**, 359-375.

16) Woodman, R. F., and Guillen, A. (1974) Radar observations of winds and turbulence of the stratosphere and mesosphere. J. Atmos. Sci. **31**, 493-505.

17) Balsely, B. B., and Gage, K. S. (1980) The MST radar techniques: potential for middle atmosphere studies. Pure Appl. Geophys. **118**, 452-493.

18) Batchelor, G. K. (1953) The theory of homogeneous turbulence. Cambridge Monographs on Mechanics and Applied Mathematics. Cambridge Univ. Press, London, p. 4 and pp. 114-132.

19) Maekawa, Y., Fukao, S., Yamamoto, M., Yamanaka, M. D., Tsuda, T., Kato, S., and Woodman, R. F. (1993) First observation of the upper stratospheric vertical wind velocities using the Jicamarca VHF radar. Geophys. Res. Lett. **20**, 2235-2238.

20) Villars, F., and Weisskopf, V. F. (1954) The scattering of electromagnetic waves by turbulent atmospheric fluctuations. Phys. Rev. **94**, 232-240.

21) Kato, S., Ogawa, T., Tsuda, T., Sato, T., Kimura, I., and Fukao, S. (1984) The middle and upper atmosphere radar: First result using a partial system. Radio Sci. **19**, 1485-1484.

22) Oliver, W. L., Fukao, S., Sato, T., Tsuda, T., Kato, S., Kimura, I., Ito, A., Saryou, T., and Araki, T. (1988) Ionospheric incoherent scatter measurements with the MU radar: Observations of *F*-region electrodynamics. J. Geomag. Geoelectr. **40**, 963-985.

23) Fukao, S., Sato, T., Tsuda, T., Kato, S., Wakasugi, K., and Makihira, T. (1985) The MU radar with an active phased array system. 1. Antenna and power amplifiers. Radio Sci. **20**, 1155-1168; Fukao, S., Sato, T., Tsuda, T., Kato, S., Wakasugi, K., and Makihira, T. (1985) The MU radar with an active phased array system. 2. In-house equipment. Radio Sci. **20**, 1169-1176.

24) Yamamoto, M., Tsuda, T., Kato, S., Sato, T., and Fukao, S. (1987) A saturated gravity wave in the mesosphere observed by the Middle and Upper atmosphere radar. J. Geophys. Res. **92**, 11993-11999.

25) Tsuda, T., Inoue, T., Fritts, D. C., VanZandth, T. E., Kato, S., Sato, T., and Fukao, S. (1989) MST radar observations of a saturated gravity wave spectrum. J. Atmos. Sci. **46**, 2440-2447.

26) Smith, S. A., Fritts, D. C., and VanZandt, T. E. (1987) Evidence for a saturated spectrum of atmospheric gravity waves. J. Atmos. Sci. **44**, 1404-1410.

27) Vincent, R. A., and Reid, I. M. (1983) HF Doppler measurements of mesosphere gravity wave momentum fluxes. J. Atmos. Sci. **40**, 1321-1333.

28) Tsuda, T., Murayama, Y., Yamamoto, M., Kato, S., and Fukao, S. (1990) Seasonal variation of momentum flux in the mesosphere observed with the MU radar, Geophys. Res. Lett. **17**, 725-728.

29) Holton, J. R., and Wehrbein, W. M. (1980) A numerical model of the zonal circulation of the middle atmosphere. Pure Appl. Geophys. **118**, 284-306.

30) Reid, I. M., and Vincent, R. A. (1987) Measurements of the horizontal scales and phase velocities of short period mesospheric gravity waves at Adelaide, Australia. J. Atmos. Terr. Phys. **49**, 1033-1048.

31) Hines, C. O. (1965) Dynamical heating of the upper atmosphere. J. Geophys. Res. **70**, 177-183.

32) Yamanaka, M. D., and Fukao, S. (1994) A simple model of gravity-wave momentum and energy fluxes transferred through the middle atmosphere to the upper atmosphere. J. Atmos. Terr. Phys. **56**, 1375-1385.

33) Vadas, S. L., and Fritts, D. C. (2004) Thermosphere responses to gravity waves: Influences of increasing viscosity and thermal diffusivity. J. Geophys. Res. (Submitted).

34) Shepherd, G. G. (2002) *In* Spectral Imaging of the

Atmosphere. Academic Press, Amsterdam-Boston-London-New York-Oxford-Paris-San Diego-San Fransisco-Singapore-Sydney-Tokyo, pp. 102-128, 191-196.

35) Fukao, S., Yamanaka, M. D., Sato, T., Tsuda, T., and Kato, S. (1988) Three-dimensional air motions over the Baiu front observed by a VHF-band Doppler radar: A case study. Mon. Weather Rev. **116**, 281-292.

36) Fukao, S., Wakasugi, K., Sato, T., Morimoto, S., Tsuda, T., Hirota, I., Kimura, I., and Kato, S. (1985) Direct measurement of air and precipitation particle motion by very high frequency Doppler radar. Nature **316**, 712-714.

37) Fukao, S., Hasiguchi, H., Yamamoto, M., Tsuda, T., Nakamura, T., Yamamoto, M. K., Sato, T., Hagio, M., and Yabugai, Y. (2003) The Equatorial Atmosphere Radar (EAR): System description and first results. Radio Sci. **38**(4), 1053, doi: 10.1029/2002RS002767.

38) Nishimura, K., Gotoh, E., Takai, T., and Sato, T. (2005) Adaptive clutter suppression for multi-static observation with Equatorial Atmosphere Radar. Proc. 2005 IEEE, International Geoscience and remote sensing symposium, Seoul, Korea, July, pp. 5104-5107.

39) Iwasaki, T., Yamada, S., and Tada, K. (1989) A parameterization scheme of orographic gravity wave drag with two different vertical partitionings. Part I: Impacts on medium-range weather forecasts. J. Meteorol. Soc. Jpn. **67**, 11-27.

40) Ecklund, W. L., Carter, D. A., and Balsley, B. B. (1988) A UHF wind profiler for the boundary layer: Brief description and initial results. J. Atmos. Oceanic Technology **5**, 432-441.

41) Hasiguchi, H., Fukao, S., Moritani, Y., Wakayama, T., and Watanabe, S. (2004) A lower troposphere radar: 1.3-GHz active phased-array type wind profiler with RASS. J. Meteorol. Soc. Jpn. **82**, 915-931.

42) Tsuda, T. (1982) Kyoto meteor radar and its application to observation of atmospheric tides. Ph. D. thesis, Radio Atmospheric Science Center, Kyoto Univ., Uji, Japan.

Profile

Susumu Kato was born in 1928 and started his research career in 1952 with studies on dynamics of the ionosphere and geomagnetism after graduating from Faculty of Science Kyoto University. He worked on dynamo theory of solar-quiet geomagnetic daily-variation and theory of atmospheric tides. His work paved the way to establish the classical atmospheric-tidal theory which has contributed significantly to the progress of meteorology. He was appointed Professor of Kyoto University in 1967. Later in 1984 he was successful to construct, in Shigaraki near Kyoto, the MU radar which remains, even now, the best facility in the world for observing atmospheric waves in the mesosphere, the stratosphere and the troposphere. He established Radio Atmospheric Science Center Kyoto University for operating the facility which has been open internationally for visiting scientists concerned. After retiring from Kyoto University to be Emeritus Professor he worked at Bandung Institute of Technology as a visiting Professor in 1994-1997 for his strong interests in teaching students about equatorial atmosphere dynamics in the Indonesia region which controls global climate on this planet. He was President of The Society of Geomagnetism and Earth, Planetary and Space Sciences in 1979-1980. In 1987 he was awarded the Appleton Prize from Royal Society of London and in 1989 the Japan Academy Prize. He was elected a Fellow of American Geophysical Union in 1991 and a Foreign Associate of National Academy of Engineering of the U. S. A. in 1995. He was a Fellow of International Institute for Advanced Studies in 1998.